HT-ATES system case study on TU Delft campus

Tess Wegman

October 23, 2017

TU Delft

Delft University of Technology

CTB3000 - Bachelor Eindwerk

HT-ATES system case study on TU Delft campus

Increasing efficiency with density difference compensation with the application of saline groundwater from deeper layers

By:
Tess Wegman
4350324

Supervisor:
Martin Bloemendal

Faculty of Civil Engineering and Geosciences

Preface

This thesis is about the effects of density difference compensation in High Temperature Aquifer Thermal Energy Storage systems. This was written in partial fulfilment of my Bachelor of Science in Civil Engineering at the Delft University of Technology.

I would like to thank my supervisor Ir. Martin Bloemendal for introducing me to this topic and helping me throughout my research. He was always being available to lead me into the right direction whenever obstacles arose. I would also like to thank Astrid van Leeuwen and all the other people who reviewed my work.

Tess Wegman

Abstract

High Temperature Aquifer Thermal Energy Storage (HT-ATES) systems can be implemented to store geothermal energy, residual industrial heat and solar heat. Due to the large temperature differences between the injection fluid and ambient groundwater, buoyancy flow occurs, which causes heat losses which in turn results in poor efficiency of such systems. The heat losses can be reduced by applying density difference compensation, this entails injection water with a higher salinity, to compensate for the low density caused by the high temperature of the injection fluid.

The goal of this study is to get insight into the behaviour of a possible HT-ATES system on the campus of the TU Delft with the injection of saline groundwater from deeper layers for storage in both less deep and less saline aquifers. To achieve this different cases will be considered; a reference case, a theoretical optimum, density difference compensation of the TU Delft case and the optimum density difference compensation. For these cases, different scenarios are modelled in SEAWAT to identify the influence of injection temperature, injection volume, aquifer thickness, and hydraulic conductivity on the behaviour of the system.

Using the density difference compensation from the aquifer at TU Delft, with a salinity of 16.4 kg/m^3, a maximum improvement of 2.0% can be achieved. Also, differences between the different scenarios for the TU Delft case were maximum 2.5%, with exception for a thicker aquifer or smaller injection volume. Due to the large injection volume in thin aquifers, the hot water has a large volume, causing conduction losses to dominate in the system. For thick aquifers a lot of density driven flow occurs in the reference case. With optimum density difference compensation, having a salinity of 39.1 kg/m^3, the density driven flow can be significantly decreased and the efficiency increased with 21.5%. Both aquifer thickness and salinity of the injection fluid have a negative correlation with salt recovery.

Thin aquifers in relation to injection volume are not sensitive to density driven flow, so density difference compensation is not useful for such HT-ATES systems. Density difference compensation in the case of the TU does give significant improvement in efficiency. The most influential parameter on the efficiency is aquifer thickness, for both the cold and warm well, in relation to injection volume. For thick aquifers with optimum density difference compensation the highest efficiency of 75.5% is achieved after 10 cycles.

Table of Contents

Preface ii

Abstract ii

List of Symbols v

1 Introduction 1

1.1 Problem description 1

1.2 Research goal 2

1.3 Approach 2

2 Aquifer Thermal Energy Storage 4

2.1 Categories 4

2.2 Challenges with HT-ATES 5

2.3 Optimisation of HT-ATES efficiency 7

3 Methods and material 9

3.1 Delft Aardwarmte Project 9

3.2 Simulation environment 10

3.3 Assessment framework 13

4 Results 14

4.1 Heat recovery efficiency 14

4.2 Salt recovery 14

4.3 Parameters 15

5 Discussion 18

5.1 Simplifications 18

5.2 Interfering systems within HT-ATES radius 18

5.3 Influencing parameters 18

5.4 Effectiveness density difference compensation over time 18

6 Conclusion and Recommendations **21**

6.1 Influencing parameters 21

6.2 Effect density difference compensation on efficiency 21

6.3 Distribution of temperature 21

6.4 Salt recovery 21

6.5 Distribution of salt 22

6.6 Recommendations 22

References **23**

Appendices **25**

Appendix A Model boundaries and parameters **25**

Appendix B Efficiency and salt recovery overview **28**

Appendix C Results: figures **30**

Appendix D Formulas **33**

List of Symbols

C_s	Solute concentration water	[kg/m^3]
c_{pf}	Heat capacity water	[J/(kg °C)]
c_{ps}	Heat capacity of solid	[J/(kg°C)]
$C_{S,a}$	Ambient groundwater salt concentration	[kg/m^3]
$C_{S,ex}$	Extracted salt concentration	[kg/m^3]
$C_{S,in}$	Injected salt concentration	[kg/m^3]
H_a	Confined aquifer thickness	[m]
L	Filter length	[m]
M	Mixed convection rate	[-]
$M_{S,ex}$	Extracted salt mass	[kg]
$M_{S,in}$	Injected salt mass	[kg]
R_T	Thermal retardation factor	[-]
S	Salinity water	[kg/m^3]
T	Temperature	[°C]
v_{forced}	Forced convection	[m/s]
v_{free}	Free convection	[m/s]
V_{in}	Injected water volume	[m^3]
T_a	Temperature ambient groundwater	[°C]
T_{ex}	Temperature extracted water	[°C]
T_{in}	Temperature injected water	[°C]
V_{ex}	Volume per time step of extracted water	[m^3]
V_{in}	Volume per time step of injected water	[m^3]
μ	Dynamic fluid viscosity	[kg/m day]
ρ	Fluid density	[kg/m^3]
$\rho(X, Y)$	Pearson correlation coefficient between two random variables X and Y	[-]
ρ_b	Bulk density	[kg/m^3]
ρ_{ex}	Density extracted water	[kg/m^3]
ρ_{in}	Density injected water	[kg/m^3]
θ	Porosity	[-]

1 Introduction

1.1 Problem description

Since the industrial revolution the human kind has been rapidly depleting the world's resources and polluting the atmosphere with greenhouse gas emissions. As a result the average global temperature has risen with 0.8 °C since 1880, according to NASA's GISS [1]. To put this into perspective; in the past a global temperature drop of between 1 and 2°C has been sufficient to cause a small Ice Age [1]. The ongoing temperature rise is having disastrous effect on ecosystems and living beings on Earth. To cut down on greenhouse gas emissions and to prevent the depletion of non-renewable resources, sustainable alternatives have to be implemented. Of the total energy consumption in the Netherlands, 40% is attributed to the generation of heat [2]; 95% of this generated heat is generated through the burning of natural gas [3].
An alternative to heating houses with natural gas, is using the more sustainable alternative: geothermal energy. Geothermal energy is heat energy from the earth. The centre of the Earth can be compared to a nuclear reactor, lots of heat is constantly being generated during the nuclear decay of naturally radioactive materials [4]. This heat reaches the Earth's crust through thermal convection and conduction. Geothermal energy can be extracted from the Earth through groundwater wells, such wells are constant sources of energy.
Due to seasonal differences, the demand will vary throughout the year, as showed in Figure 1.1. To compensate for this, thermal energy has to be stored during low demand, so that in winter, demands can be met. Besides storing geothermal energy in HT-ATES systems, such systems can serve a wider application, residual industrial heat and solar heat can be stored in HT-ATES systems.

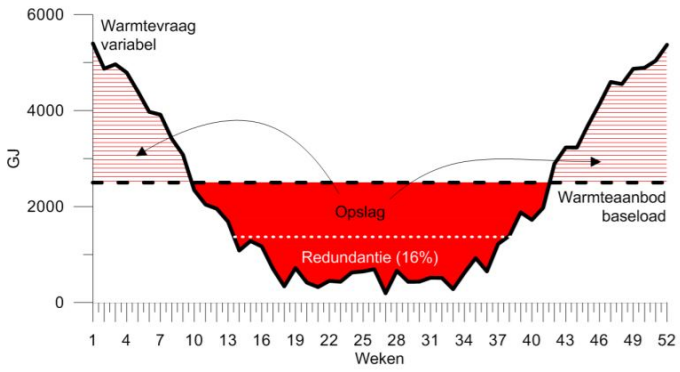

Figure 1.1: Seasonal variation in heat demand, the mismatch of demand and supply. (Hartog et al. [5]).

However, storing heat at temperatures higher than 60 °C is not common in practice and requires more investigation in order to become economically viable and to open the possibility of widespread implementation.
Heat can be stored in aquifers, which are permeable water bearing soil layers. Within these Aquifer Thermal Energy Storage (ATES) systems two main categories can be distinguished, defined by the temperature of the stored water. Low temperature storage (LT-ATES), with temperatures lower than 30 °C, and high temperature storage (HT-ATES), with temperatures above 60 °C (see figure Figure 1.2). In the Netherlands LT-ATES systems are widely used, however, there are currently no operating HT-ATES systems [6]. Storing water of temperatures above 60 °C is complex, making it very challenging to operate HT-ATES systems cost

effectively; this explains the lack of HT-ATES systems in the Netherlands.

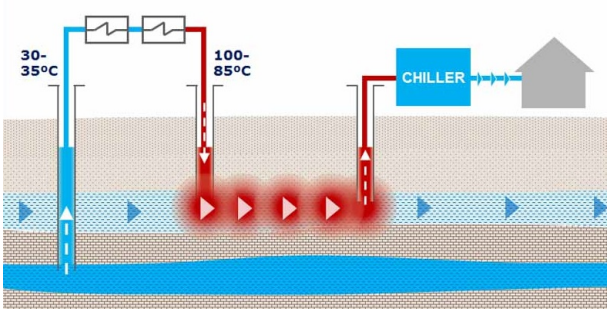

Figure 1.2: High Temperature Aquifer Thermal Energy Storage. (GFZ [7]).

From the relatively large temperature difference between the hot stored water and the colder ambient groundwater follows a difference in density. The injected hot water has a smaller density than the cold ambient groundwater, causing the hot water to rise. This has a negative influence on the recovery temperature efficiency. Not all the risen hot water can be recovered again by the well. Furthermore, extra temperature losses will occur due to increased conduction and free thermal convection.
Theoretically the efficiency of the system can be significantly increased if the density difference could be compensated for. A possible method for density difference compensation, is using water with a higher salinity, thus a higher density, as injecting fluid, like the method of Van Lopik et al. [8]

1.2 Research goal

The goal of this study is to get insight into the behaviour of a possible HT-ATES system on the campus of Delft University of Technology (TU Delft) with the injection of saline groundwater from deeper layers for storage in both less deep and less saline aquifers over several cycles. The following sub- questions will be answered:

- Which parameter or parameters does/do most significantly influence the efficiency and salt recovery of the well?
- How does density difference compensation influence the thermal recovery efficiency for the different scenarios?
- How is the distribution of temperature in space around the well after several cycles for different cases?
- How does salt recovery differ for different cases and scenarios and how does this affect density difference compensation over time?
- What is the distribution of salt in space around the well after several cycles for different cases?

1.3 Approach

To get an insight into the behaviour of HT-ATES systems with density difference compensation, first a general introduction to ATES systems is given in Chapter 2. The challenges that arise when storing high temperature water are presented in Section 2.2.
To model the behaviour of HT-ATES system, SEAWATv4 is used. In Chapter 3 all elements of the simulation are explained. In this study the case of a HT-ATES system on the campus of

TU Delft is used. First the parameters and boundaries of the system at TU Delft are defined. In Section 3.3 the assessment framework is defined in order to properly interpret the results. This is followed by a case study, including a reference case, a theoretical optimum and the case with density difference compensation. These cases are considered for several scenarios, to investigate the influence of certain parameters on the system. This provides insight into the different conditions. The results are presented in Chapter 4.
Finally the results are discussed, and optional improvements for the study brought forward. Conclusions are drawn about the behaviour and thus the feasibility of the HT-ATES system with density difference compensation.

2 Aquifer Thermal Energy Storage

This chapter provides background information about (HT-)ATES systems. Firstly, different categories of ATES systems are briefly introduced, secondly the challenges with HT-ATES will be explained. And lastly, parameters which can optimise the efficiency of HT-ATES systems are discussed.

2.1 Categories

Heat can be stored in aquifers, which are permeable water bearing soil layers. Within these Aquifer Thermal Energy Storage (ATES) systems different categories can be distinguished, an overview is provided in Figure 2.1. As mentioned in the Introduction, a difference can be considered based on storage temperature: low temperature storage (lower than 30 °C), and high temperature storage (above 60 °C). LT-ATES are usually situated in shallow aquifers (50-250m deep) and HT-ATES in deep aquifers (deeper than 500m). Furthermore, a difference based on the number of boreholes can be considered, monowells and doublets. The next sections further elaborate on the differences between high and low temperature storage and the differences between monowells and doublets.

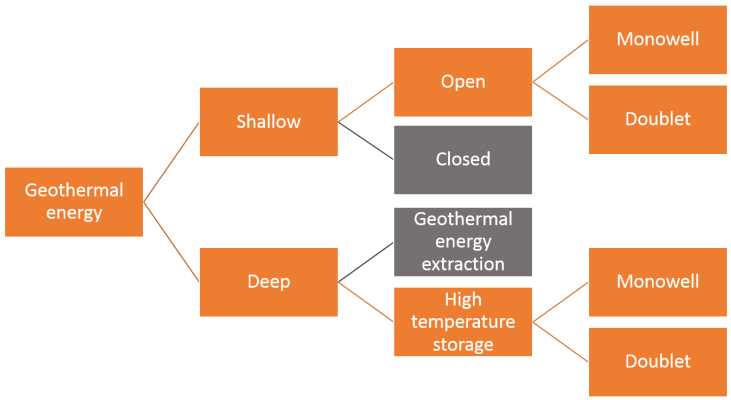

Figure 2.1: Categories within ATES systems. (based on Cahier Bodemenergie [9]).

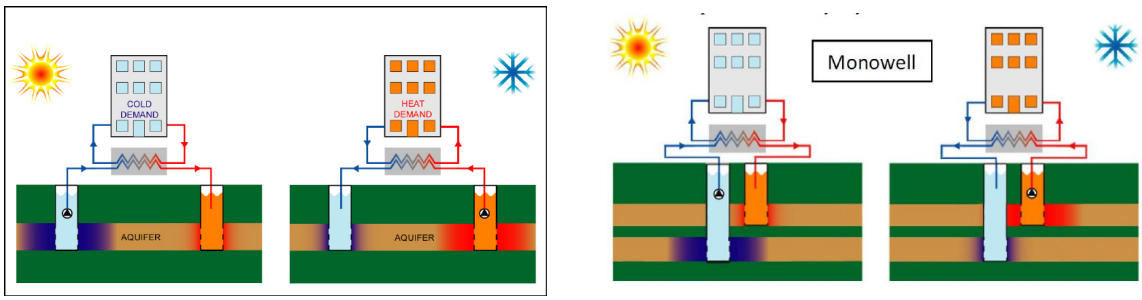

(a) Doublet

(b) Monowell

Figure 2.2: Schematization doublet and monowell. (Calje [10]).

2.1.1 Monowell and doublet

Shallow ATES systems are usually heat and cold storage systems. If cold and hot water are both extracted and injected by the same well at different depths, this is a monowell (see Figure 2.2b).

The cold and hot storage are separated by a vertical distance from each other, usually with a difference between 5 and 30 metres [9]. Cold and hot storage are usually situated in the same aquifer, in order to prevent mixing relatively small discharges should be used, around 50 m^3/h. A doublet consists of two wells (see Figure 2.2a), with a horizontal distance between the cold and hot storage. Doublets allow a significantly larger discharge, up to 250 m^3/h, this makes doublets generally more suitable for bigger buildings.

2.1.2 LT-ATES and HT-ATES

The differences between LT-ATES and HT-ATES systems can be directly linked to the storage temperature. The water from LT-ATES systems is not hot enough to use as an immediate source of energy, to heat buildings. To generate sufficient heat to do so, a heat pump is required. Such pumps require electrical energy to operate, which means LT-ATES systems alone cannot generate enough energy to heat buildings. Well functioning HT-ATES systems do not require a heat pump. Another advantage of storing at high temperature is that, with the same volume, a larger amount of energy can be stored than with the same volume of colder water.
Theoretically HT-ATES systems have a higher potential than LT-ATES, because HT-ATES systems do not require a highly energy consuming heat pump. Nonetheless, the LT-ATES systems are widely used in the Netherlands, and on the contrary, there are currently no operating HT-ATES systems in the Netherlands [6]. The reason for this is that higher temperature recovery efficiencies can be achieved with LT-ATES systems than with HT-ATES systems. More on temperature recovery efficiency can be found in Section 2.2.

2.2 Challenges with HT-ATES

Doughty et al. [11] described the four processes which cause energy losses in HT-ATES systems; thermal conduction, dispersion, regional groundwater flow and density driven flow. Dispersion is the measure of deviation of the single water particles from the average flow. Dispersion is not dependent on temperature, so it does not influence the efficiency difference between HT-ATES and LT-ATES systems.
Injection temperature is linearly proportional to heat loss due to thermal conduction. However, injection temperature does not affect thermal recovery efficiency. This is because thermal energy efficiency is defined as the ratio between lost heat and the total injected heat. With a higher injection temperature the heat loss due to thermal convection will increase with the same rate. Since both factors increased proportionally, the thermal efficiency coefficient will remain constant. So heat loss due to thermal conduction is not influencing the thermal recovery efficiency [12].
The main factor, negatively influencing thermal recovery efficiency, is density driven flow. To further explain this, the three different operation stages of HT-ATES systems will be considered. Firstly, hot water is injected into the aquifer, secondly, the water is stored in the aquifer, and finally, the hot water is extracted again.
During the injection stage, hot water is pumped into the aquifer, as can be seen in Figure 2.3a. From the large temperature difference between the injected water and the ambient groundwater, follows a difference in density. The injected water has a smaller density than the ambient groundwater, as a result buoyancy forces cause hot water to flow upwards, as illustrated in Figure 2.3b. This upward flow is called density driven flow. The hot water rising to the top of the aquifer results in a reversed conical shape. This tilted front allows more heat losses, and the steeper this front gets, (so a bigger angle with the vertical line,) the more heat losses occur. These enhanced heat losses are caused by several factors. The tilted front results in a bigger area in contact with the top confining layer, allowing more heat loss due to conduction (this conduction does have a negative effect on the heat recovery efficiency). Secondly, the tilted front has a larger area, allowing more free thermal convection (indicated by the arrows in Figure 2.3a

and Figure 2.3b), which is the transfer of heat caused by the movement of water. Finally, the risen hot water cannot all be recovered by the same well during the recovery phase, which leaves a hot water volume behind, as Figure 2.3c is showing. Instead, part of the cold water (blue) will be extracted.

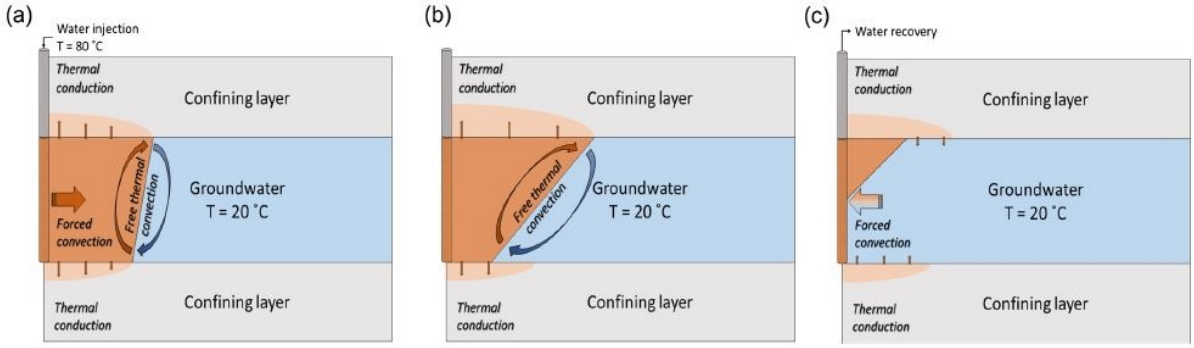

Figure 2.3: Schematic overview of a full HT-ATES recovery cycle in a confined aquifer for (a) injection, (b) storage and (c) extraction periods. (Van Lopik et al. [8]).

In a study by Ward et al. [13], the smallest tilting angle was found for fast injection rates and small hydraulic conductivities during the injection stage. For the storage phase, a longer storage duration causes a bigger tilting angle. And as well as during the injection phace, hydraulic conductivity has a similar influence on tilting angle. For the recovery phase, similarly to the injection phase, faster pumping leads to a smaller tilting angle.
To understand the reason why pumping rates influence the tilting angle, free and forced convection are introduced. Free convection is water flow caused by density differences and forced convection is the water flow caused by a hydraulic gradient, which occurs while pumping. The ratio between forced convection (v_{forced}) and free convection (v_{free}) can be defined as the mixed convection rate (M), see Equation 2.1.

$$M = \frac{v_{free}}{v_{forced}} \tag{2.1}$$

If forced convection is dominant (M<<1), free thermal convection has negligible influence on water flow, thus no tilted front will occur; this can be seen in Figure 2.4a. In Figure 2.4b, which shows a mixed convective regime, a tilted front can be seen. In this case density driven flow does have an influence on water flow.

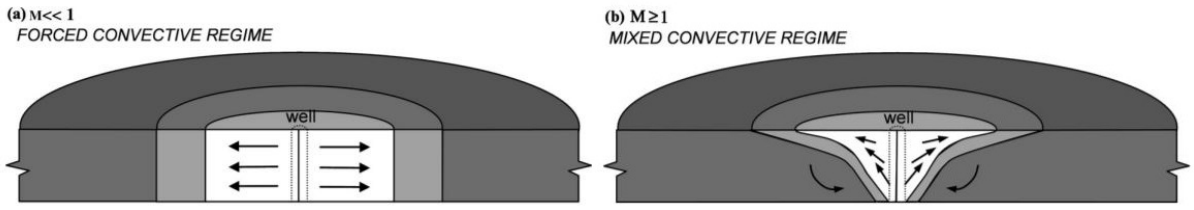

Figure 2.4: Forced and mixed convective regime. (Ward et al. [13]).

2.3 Optimisation of HT-ATES efficiency

2.3.1 Injection volume and aquifer thickness

In theory the highest efficiency, regarding injection volume and aquifer thickness, can be achieved when the shape of the water volume has the smallest area. Spheres have the smallest possible surface area for a given volume, so the highest efficiency can be expected when the shape of the water bubble is nearest to the shape of a sphere. The smallest volume will have the smallest possible amount of conduction and free thermal convection.
Area (A) and injected volume (V_{in}) can both be expressed in filter length (L) and thermal radius (r_{th}) [14], see Equation 2.2:

$$\frac{A}{V_{in}} = \frac{2\pi r_{th}^2 + 2\pi r_{th} L}{\pi r_{th}^2 L} = \frac{2}{L} + \frac{2}{r_{th}} \tag{2.2}$$

with the thermal radius being defined according to Equation 2.3 [8], with H_a aquifer thickness, θ porosity and R_T thermal retardation factor:

$$r_{th} = \sqrt{\frac{V_{in}}{\pi H_a \theta R_T}} \tag{2.3}$$

The thermal retardation factor is defined as: [8]

$$R_T = 1 + \frac{\rho_b}{\theta} \frac{c_{ps}}{\rho_f c_{pf}} \tag{2.4}$$

with ρ_b and ρ_f being bulk density and water density, c_{ps} heat capacity of solid, and c_{ps} and c_{pf} heat capacity of solid and heat capacity of water.
Next, area over volume ($\frac{A}{V_{in}}$) can be plotted for several volumes to find the optimum filter lengths. The optimum filter length will occur when the area is smallest with respect to the volume, so when $\frac{A}{V_{in}}$ has its minimum. An example plot is given in Figure 2.5.

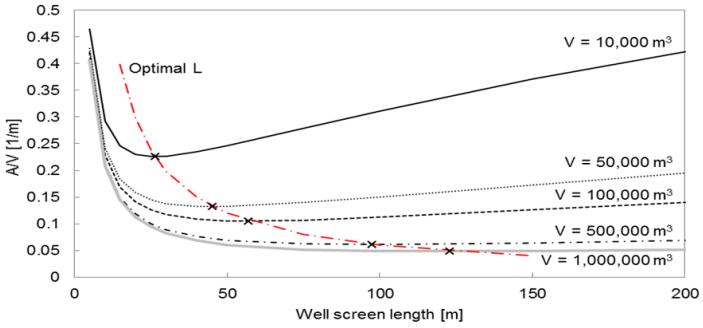

Figure 2.5: Optimum well screen lengths by given injection volumes. ([14]).

2.3.2 Temperature and salinity

The density of water is dependent on both temperature and salinity. In Figure 2.6 the density of water as function of salinity and temperature is given. Here it can be seen that for ambient groundwater of 14.4 °C and salinity of 9.6 kg/m^3, water with an injected temperature of 70 °C reaches the optimum density difference compensation with a salinity of 39.1 kg/m^3. In case

the of the TU Delft, the salinity of the injected water is 16.4 kg/m^3, which gives a significantly lower density than the ambient groundwater with the applied injection temperature of 70 °C.

2.3.3 Density difference compensation with groundwater from lower layers

Density difference compensation can be applied with saline groundwater from deeper layers. For such HT-ATES systems monowells can be implemented. Saline water can be extracted from a deeper aquifer, and injected into a shallower aquifer, the shallow aquifer functioning as the high temperature storage. Because the saline well is situated in a different aquifer than the hot storage, significantly higher pumping rates than 50 m^3/h (as mentioned in Section 2.1.1) can be used for this application of monowells.

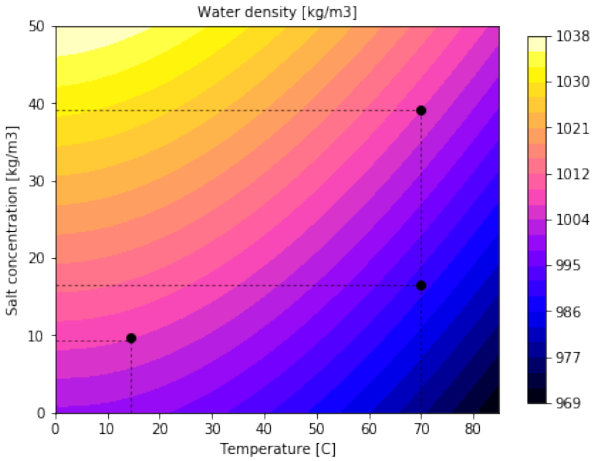

Figure 2.6: Density of water as function of salinity and temperature.

3 Methods and material

In this chapter the research setup is discussed. First the case study and previous research results will be presented. Furthermore, the simulation environment will be introduced briefly, including the modelled cases and scenarios. Finally, the assessment framework will define a context to interpret the results well.

3.1 Delft Aardwarmte Project

The 'Delft Aardwarmte Project' (Delft Geothermal Project), was founded in 2008, to provide a sustainable heat source at the TU Delft. The goal is to install a geothermal well at the TU Delft campus [15]. The current objective is to have several monowells to inject water with a temperature of 70 °C. This case is further used throughout this study.
Van Lopik et al. [8] has shown that a significantly higher recovery temperature efficiency can be achieved by minimising the buoyancy forces, and thus the negative results of these explained in Section 2.2. This can be done by increasing the salinity of the hot water injected in the warm well, thus compensating the density differences. Van Lopik et al. [8] investigated the theory of density difference compensation. In practice, the more saline water can be extracted from deeper situated soil layers, because salinity of groundwater increases with depth.
Leclercq [16] has shown analytically that this application of density difference compensation could successfully be implemented for the case at TU Delft, based on the feasibility study which Hacking [17] has done.
Hacking studied the feasibility of a HT-ATES on the campus. This study found that the required energy capacity for an HT-ATES system TU Delft lies between 100,000 and 200,000 GJ, the corresponding injection volume is between $9.55{\cdot}10^5$ and $3.18{\cdot}10^6$ m^3 (depending on the temperature difference between extracted and injected water and interval for energy demand). A layer that could be suitable for high temperature storage is the top part of the Maassluis Formation. This aquifer has a thickness of about 20m, the top is situated at a depth of 160m, the horizontal permeability lies between 10 and 100 m/d and the vertical permeability lies between 0.001 and 1 m/d. This aquifer will be referred to as the warm well in the rest of this report.
From Hacking's study, Leclerq [16] deduced that the most suitable layer to extract saline water from, is the Texel greensand member. This aquifer is situated at a depth of 560m, going down with a thickness of 20m. This aquifer has a hydraulic conductivity of 15mD. This aquifer will be referred to as the 'cold' well in the rest of this report.
Leclercq (2017) also gave an insight in the temperature and salt gradients in Delft. The first 100m are assumed to have a constant temperature of 13 °C, and after 100m the temperature gradient is 20 °C/km. The salt gradient in Delft is 17 mg/L/m after 150m. For the first 150m the salinity gradient can be described by Equation 3.1, with z being the depth in metres.

$$S_{gradient} = 1.7667 \cdot \ln(z) - 4.6622 \qquad for\ z > -150m \tag{3.1}$$

Hacking and Leclercq made progress in the research of implementing an HT-ATES at campus. However, the effect of density difference compensation on efficiency, recovery temperature and distribution of salt and heat around the well have not been investigated yet.

3.2 Simulation environment

The behaviour of the aquifers is modelled in SEAWATv4. This is a combination of MT3D and MODFLOW. Seawat combines the MT3D and MODFLOW packages in order to simulate variable density groundwater flow and solute and heat transport.
Both salt concentration and temperature influence fluid viscosity and fluid density. In SEAWATv4, equations of state are used to express viscosity and density as functions of salt content and temperature [8].
Fluid viscosity (μ) is given by Equation 3.2:

$$\mu(C_s, T) = 2.394 \cdot 10^{-5} \cdot 10^{\left(\frac{248.37}{T+133.15}\right)} + 1.923 \cdot 10^{-6}(C_s) \tag{3.2}$$

with T being the temperature of water and C_s the solute concentration of water.

Fluid density (ρ) is given by Equation 3.3:

$$\begin{aligned}\rho(T,S) =&(999.9 + 2.034 \cdot 10^{-2}T - 6.162 \cdot 10^{-3}T^2 + 2.261 \cdot 10^{-5}T^3 - 4.657 \cdot 10^{-8}T^4)+ \\ &(802.0\frac{S}{1000} - 2.001\frac{S}{1000}T + 1.677 \cdot 10^{-2}\frac{S}{1000}T^2 - 3.060 \cdot 10^{-5}\frac{S}{1000}T^3 - \\ &1.613 \cdot 10^{-5}\left(\frac{S}{1000}\right)^2 T^2)\end{aligned} \tag{3.3}$$

with S, being the salinity of water.

The dependency of water density (ρ) on temperature (T) is not a linear function, which can be seen in Figure 3.1. SEAWAT uses a linearization between two points for the $d\rho/dT$ relation.

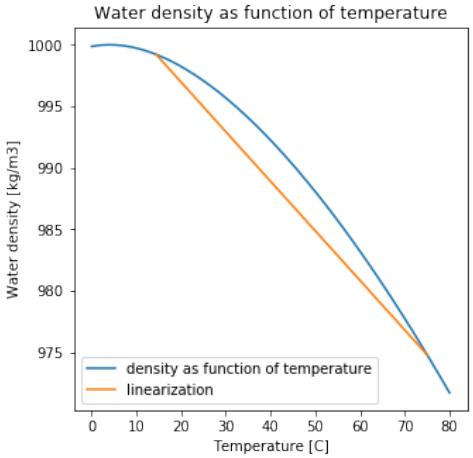

Figure 3.1: Water density as function of temperature

3.2.1 Parameters and boundaries

An overview of all parameters and boundaries can be found in the tables of Appendix A. In this section some parameters and boundaries are clarified.

Model boundaries

Axi-symmetric flow around the well is considered, so an cylindrical coordinate system is used of which an example is given in figure Figure A.1. In z direction the aquifers and aquitards are defined, this is a simplification of reality. In Figure 3.2a the soil layers are shown how they are in

reality, according to Hacking (2017). In Figure 3.2b the simplification which will be used in the simulation is shown. This simplification is used to reduce the calculating time. The Maassluis formation aquifer, of which the top is situated at a depth of 160 metres, is modelled at -10 metres. The overlying aquitard is considered to start at z=0 till z=-10. All layers between the Maassluis formation (hot well) and Texel greensand member ('cold' well), are modelled as one single aquitard with a thickness of 50m, situated between -30m and -80m. The actual distance between the bottom of the Maassluis formation and top of Texel greensand member is 380m.

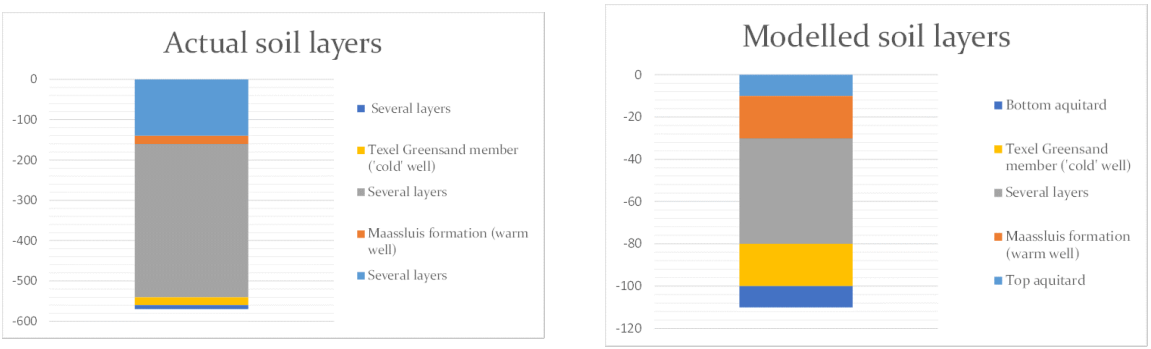

(a) Actual soil layers

(b) Modelled soil layers

Figure 3.2

Aquifer and aquitard properties

The salinity of the aquifers and aquitards is calculated according to the salinity gradients Leclercq found, mentioned in Section 3.1. For both aquifers a constant salinity is considered, based on the salinity in the middle of the aquifer. For the layers between the two aquifers, a linearly increasing salinity is assumed. The salinity distribution is shown in a plot in Figure A.2 in Appendix A. The ambient temperatures are calculated with a temperature gradient of 20 °C/m, considering a constant temperature of 13 °C for the first 100 metres.

Groundwater properties

A linearization is made for $d\rho/dT$, which is the change in water density per change in temperature. A linearization between 14 °C and 75 °C is made, so the corresponding $d\rho/dT$ of -0.40 is chosen.

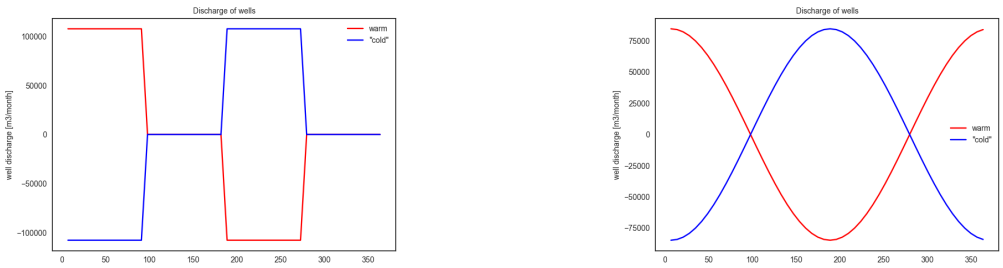

(a) Block function

(b) Sinusoidal function

Figure 3.3: Flow regimes

Flow regime

Different flow regimes can be considered. The first one being a block function, like in Figure 3.3a. This considers four seasons per year of 91 days. During the first season hot water will be injected in the well, the second season is a storage phase, the third season hot water will be extracted and the fourth season is a rest phase. Secondly, a more gradual flow regime can be used. The discharge follows a sinusoidal pattern, like in Figure 3.3b. With this flow regime there are no long periods without forced flow. In this study a block function is used to determine the flow regime.

3.2.2 Case study

To get a good insight in the influence of density difference compensation cases A, B, C and D will be considered in the case study section of the simulation:

- **A. Regular setup (reference)**
  The regular setup is the case without density difference compensation, this is the 'worst-case scenario'. In this scenario the injected hot water will contain the same salinity as the salinity of the groundwater in the Maassluis aquifer. In the model all the soil layers get the same salinity assigned to them as the actual salinity of the Maassluis aquifer.
- **B. Density difference compensation from case study**
  The case of density difference compensation, using saline water, is the case that will be used in practice at TU Delft. Water from the deeper situated (-560 till -580 m) Texel greensand aquifer, will be used as injection water for Maassluis formation (-160 till -180m), which is the water storage aquifer. The deeper situated Texel greensand aquifer has water with a higher salinity, and will thus be able to (partially) compensate for the density difference.
- **C. Theoretical condition of no free thermal convection (optimum)**
  The (theoretical) case neglecting free thermal convection, is used as a reference. In theory the thermal energy coefficient could become as high as the outcome as this case with density difference compensation. This optimum case is reached by enabling the viscosity and density driven flow functions in SEAWAT.
- **D. Optimum density difference compensation**
  Since salinity of the TU Delft case (case B), is way lower than the required salinity for optimum density difference compensation, this additional case with an optimum salinity of 39.1 kg/m^3 is considered.

3.2.3 Scenarios

Different scenarios will be considered to get an insight in the influence of certain parameters of the system. Since the soil parameters are not exactly known at the TU Delft yet, it is useful to get an insight in different scenarios between the known range. Furthermore differences between the different cases could be discovered.
Eleven different scenarios are considered, a base scenario and ten scenarios with one or two varying parameter(s) with respect to the base scenario. Those eight scenarios will have varying injection volume (V_{in}), injection temperature (T_{in}), aquifer thickness (H_a), flow regime, vertical hydraulic conductivity (K_v) and horizontal hydraulic conductivity (K_h). The parameters of injection volume and hydraulic conductivity will lie between the ranges of values found by Hacking (2017). Range of K_h is 10 - 100 m/d and the assumption that K_v is $\frac{K_h}{10}$-$\frac{K_h}{2}$. For the injection volume the estimated volume necessary for the TU Delft is between $9.55 \cdot 10^5$ and $1.91 \cdot 10^6$ m^3, when assuming a dT of 25 degrees. The base scenario will have an average of the

volume range and one of the scenarios will assume the lowest volume divided by 4, assuming 4 injection wells at significant difference from each other. The assumed temperature is 70, so a difference of 20 degrees colder and hotter is chosen. Since the aquifers in the case of TU Delft is very thin, a medium and large thickness of 50m and 120m are chosen for the warm well, leaving the thickness of the cold well 20m. Furthermore, one scenario has thick aquifers of 120m for both the cold and warm well. Finally a sinusoidal flow regime is chosen for two scenarios, one with all other parameters equal to the base scenario, and one scenario with a warm aquifer of 120m. An overview of the scenarios of the sensitivity analysis can be found in Table A.6.

3.3 Assessment framework

3.3.1 Thermal recovery efficiency and heat distribution

The main aspect to assess HT-ATES systems is the thermal recovery efficiency. This thermal recovery efficiency (ε_H) gives which ratio of the total injected heat (Q_{in}) is recovered after extraction (Q_{ex}), this gives the following expression:

$$\varepsilon_H = \frac{Q_{ex}}{Q_{in}} = \frac{\sum [V_{ex} \cdot \rho_{ex}(T,S) \cdot c_{pf} \cdot (T_{ex} - T_a)]}{\sum [V_{in} \cdot \rho_{in}(T,S) \cdot c_{pf} \cdot (T_{in} - T_a)]} \tag{3.4}$$

in which $V_{in,ex}$ are the injected and extracted volumes, $T_{in,ex}$ are the injected and extracted temperatures, T_a is the temperature of the ambient groundwater, c_{pf} is the heat capacity of water, and $\rho_{in,ex}$ are the densities of the injected and extracted water.
Besides the thermal recovery efficiency it is crucial to get an insight in the distribution of temperature in and around the aquifers.The distribution of heat within the aquifer has effect on the recovery temperature. The thermal radius is a measure for the spreading of the heat in the aquifer. This should be taken into account, because other heat and cold storage systems should not lie within the thermal radius of the HT-ATES system.

3.3.2 Recovery temperature

Not only the thermal recovery efficiency, but also the actual temperature of the recovered water is important. This has to be at least 40 °C, to be able to heat buildings on a cold winter day.

3.3.3 Salt recovery efficiency and salt distribution

The recovery of salt mass (ε_S) is a crucial aspect in this study, this gives an indication of the long-term effects of density difference compensation. The salt mass recovery efficiency is defined as the ratio between the total injected salt mass ($M_{S,in}$) and the total recovered salt mass after extraction ($M_{S,ex}$):

$$\varepsilon_s = \frac{M_{S,ex}}{M_{S,in}} = \frac{\sum [V_{ex} \cdot (C_{S,ex} - C_{Sa})]}{\sum [V_{in} \cdot (C_{S,in} - C_{S,a})]} \tag{3.5}$$

with $C_{S,in/ex}$ the injected and extracted salt concentrations and $C_{S,a}$ the ambient groundwater salt concentration.
The spreading of salt concentrations in both aquifers and the salinity recovery are interesting parameters in HT-ATES systems using density difference compensation. If the salt cannot be extracted well enough from the warm well, this results in salinization of the aquifer. In the long run the density difference might not be able to be compensated for by salinity.

4 Results

First the results linked to density difference compensation and salt recovery will be discussed; these results are the most insightful as regards the behaviour of the HT-ATES systems in the different cases. Secondly, the influence of the varying parameters are presented, highlighting the main differences between the scenarios. In the table in Appendix B a full overview of efficiencies and salt recoveries for the different cases can be found.

4.1 Heat recovery efficiency

The base scenario (1) was simulated for the reference case (A), with density difference compensation from the TU Delft case (B), the theoretical optimum (C) and for an optimum density difference compensation (D). There was hardly any difference in efficiency between the cases, the maximum improvement was found for the theoretical optimum ($\Delta\varepsilon_H$=0.7%) with respect to the reference case. In a very thin aquifer in comparison to the injection volume (i.e. a large A/V ratio) the thermal radius becomes very big, so the areas in contact with the overlying and underlying aquitards become very large, as can be seen in Figure 4.4. In this case thermal conduction losses become dominant over thermal convection losses and thus hardly any improvement can be made with density difference compensation.
The density difference compensation with the salinity found in the Texel greensand member (scenarios of case B) did not give any significant improvement in efficiency compared to the reference case without density difference compensation (scenarios of case A). There were no efficiency improvements above 1.0%. Furthermore, hardly any difference was found between the cases A and B for the difference between the base scenario and the other scenarios. This means that the small density difference compensation does not make the system less sensitive to parameter changes. The lack of improvement for scenarios of case B can be explained by the fact that in this case study the density difference compensation is much lower than the optimum density difference compensation, making the density difference negligible.
To show potential improvement the theoretical optimum (case C) was simulated for some scenarios with a lower A/V ratio; q small volume (scenario 4), a thick warm well aquifer (scenario 7) and thick warm and cold well aquifers (scenario 11). The most significant improvement with respect to the reference case (A) was found for the scenarios with thick aquifers ($\Delta\varepsilon_H$=33.4% and $\Delta\varepsilon_H$=33.2%).

4.2 Salt recovery

The salt recovery for the reference case (1B) is 93.6%, cases 2B, 3B, 5B, 5B and 9B also lie between 93% and 95%. This means that change in temperature, change in hydraulic conductivity and a sinusoidal flow regime have hardly any influence on salt recovery($|\Delta\varepsilon_S|$=1.1%). A medium aquifer, a thick aquifer and a smaller volume show the most significant decrease in salt recovery. With a higher injection salinity (cases D) a lower salt recovery between a range of 78% and 87% is achieved. When the thickness of the aquifer of the cold well is increased, a slightly higher salt recovery can be achieved ($\Delta\varepsilon_S$=1.9%).

4.2.1 Correlation salt recovery and efficiency

The correlation coefficient between efficiency and salt recovery for case B $\rho(\varepsilon_H, \varepsilon_S)$=0.90 was found, which belongs to a positively nearly linear correlation. This correlation was found with the Pearson correlation coefficient ($\rho(X, Y)$), which is defined as Equation D.1 in Appendix D. For case D the correlation efficiency is 0.4. For case D less scenarios are simulated, but the

correlation for case B between the same scenarios as simulated for case D is still 0.84. So for case B there is a strong positive correlation between salinity recovery and efficiency, however when the salinity is very high there is no such correlation. When the heat recovery is small, generally a lot of density driven flow occurs. In this case more salute transport takes place, due to thermal retardation the salt travels further than the hot water volume, so not all salt can be recovered.

4.2.2 Correlation salt recovery and aquifer thickness

The main variation in salt recovery and thermal heat recovery efficiency are both found within the different cases of a thick aquifer and in the difference between a thick aquifer and other scenarios (Section 4.3.1). This observation is in line with the correlation coefficient between salt recovery and aquifer thickness of case B and D, $\rho(\varepsilon_H, H_a)$=-0.89 and $\rho(\varepsilon_H, H_a)$=-0.98. In thick aquifers more density driven flow can occur, which causes more solute transport. Additionally, in a thick aquifer and for higher injection salinities, salt is more likely sink to the bottom, which makes a higher part of it unrecoverable. This explains the negative correlation between aquifer thickness and salt recovery and the lack of pronounced correlation between the salt recovery and efficiency in case D.

4.3 Parameters

4.3.1 Aquifer thickness

A thick aquifer without density difference compensation (case 7A), has the lowest efficiency of all scenarios, 53.9%. This is much lower ($\Delta\varepsilon_H$=-20%) than the base scenario. However, as mentioned in Section 4.1, for the theoretical optimum a thick aquifer can reach the highest efficiency, which is 11.9% higher than the base scenario (1C). In Figure 4.1b the theoretical optimum can be seen. In a thick aquifer, the area in relation to the volume (A/V) can stay relatively low, in comparison to the same injection volume in a thin aquifer, like in Figure 4.4, where a very big area occurs. With such big areas a lot of conduction losses will take place, regardless of the amount of density driven flow. In a very thick aquifer the heat losses due to density driven flow are significant, as can be deduced from Figure 4.1a, this causes the low efficiency for the case without density difference compensation. However, when an optimum case can be achieved, as with the theoretical optimum in Figure 4.1b, the efficiency can become higher than with a thin aquifer, because conduction losses are minimal. When the aquifers of both the warm and the cold well are big, a higher efficiency (ε_H=75.5%) can be achieved, than if just the warm well aquifer is thick ((ε_H=59.3%), as explained in Section 5.4. For both case B and D a thick aquifer has the lowest salt recovery, of $\Delta\varepsilon_S$=-4.9% and $\Delta\varepsilon_S$=-8.2% with respect to the base scenario.

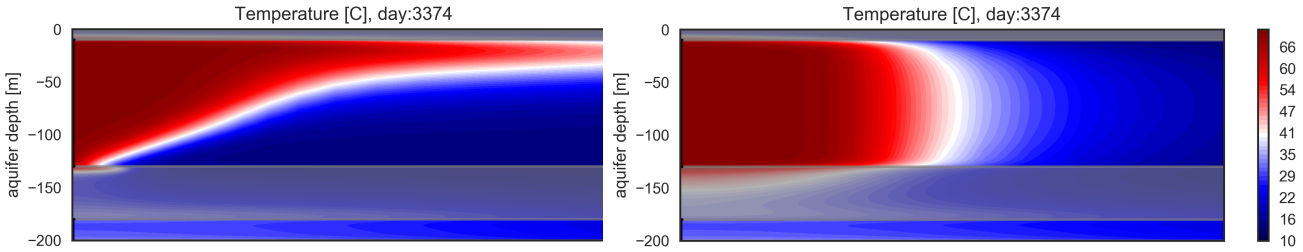

(a) Scenario 7A (b) Scenario 7C

Figure 4.1: Difference in density driven flow between reference and theoretical optimum, the shaded areas are aquitards.

4.3.2 Injection volume

A smaller injection volume (scenario 4), gives a slightly lower efficiency ($\Delta\varepsilon_H$=-7.0%) than the reference case. This is because the A/V ratio increases, so more density driven flow can occur. With a small volume some improvement can be potentially made, because case 4C had a slightly higher efficiency ($\Delta\varepsilon_H$=7.0%) than 4A. However, the actual theoretical maximum efficiency for a small volume is smaller than that of the base scenario, which makes a big volume favourable. Figure 4.2 shows that for a small volume (Figure 4.2a), a bigger ratio of the total area is in contact with the cold ambient groundwater in relation to the heated up confining aquifers. The salt recovery with a small volume is slightly lower ($\Delta\varepsilon_S$=-2.9%) than that of the base scenario.

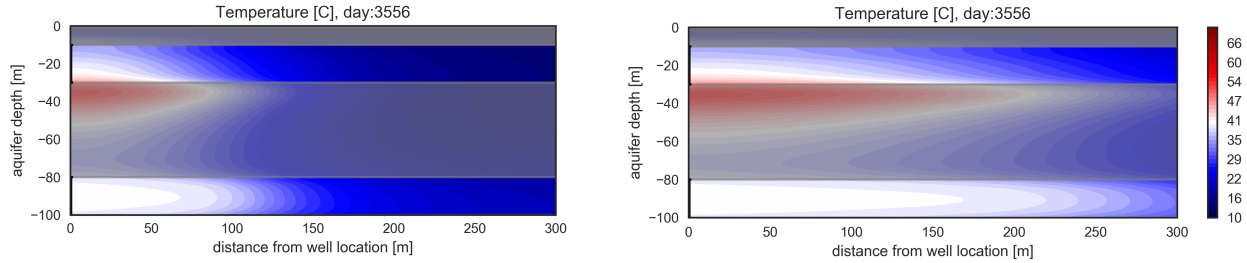

(a) Scenario 4C (b) Scenario 1C

Figure 4.2: Different injection volumes

4.3.3 Injection temperature

A higher injection temperature (scenario 2), gives a slightly smaller efficiency ($\Delta\varepsilon_H$=-2.0%) and a lower injection temperature (scenario 3) gives a slightly higher efficiency ($\Delta\varepsilon_H$=2.5%). In this case a lower temperature seems more favourable, however a smaller injection temperature will also cause a lower extraction temperature as shown in Figure 4.3.

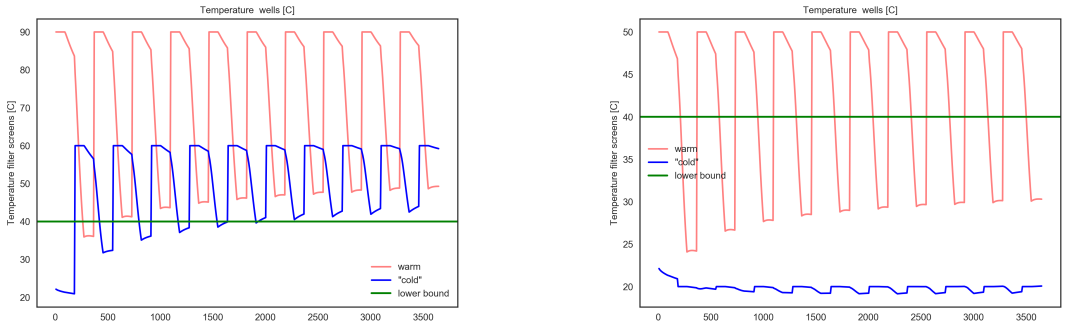

(a) Scenario 2B (b) Scenario 3B

Figure 4.3: Difference extraction temperature due to injection temperature

With an injection temperature of 90 °C, the extraction temperature will be above the lower boundary of 40 °C after one year, whilst the extraction temperature is still below the lower bound after 10 years. Figure 4.3 also shows that the extraction temperature increases for the first 5 years and stabilises there after, so with an injection temperature of 50 °C the lower bound will never be met. For the base scenario with an injection temperature of 70 °C the limit of 40 °C is met of most days of the years, as can be seen in Figure C.4 in Appendix C. There was no

significant difference ($\Delta\varepsilon_S$ <0.2%) in efficiency with or without density difference compensation, which means no difference between cases 2A & 2B and 3A & 3B. Nor did temperature have a noticeable influence on salt recovery ($|\Delta\varepsilon_S|$ <0.4%).

4.3.4 Hydraulic conductivity

A bigger hydraulic conductivity in both vertical and horizontal directions (scenario 5), gives a sightly smaller efficiency. Conversely, a smaller hydraulic conductivity in both directions (scenario 6), gives a slightly higher efficiency. The correlation between hydraulic conductivity and efficiency can be explained by the fact that with a small vertical hydraulic conductivity there is more resistance to upward flow, which will reduce the effects of density driven flow. Also the reduced resistance to horizontal flow, as a result of a low K_h, causes the water to flow less in the horizontal direction, keeping the area of the hot water smaller, and as a result less losses due to thermal conduction can take place. In Figure 4.4b, it can clearly be seen that less density driven flow has taken place than in Figure 4.4a. However, both the efficiency increase and decrease with respect to that of the base scenario found within the possible case of the TU Delft are very small (resp $\Delta\varepsilon_H$=1.3% and $\Delta\varepsilon_H$=-1.3%). Hydraulic conductivity between the researched ranges has hardly any influence on salt recovery ($|\Delta\varepsilon_S|$ <0.4%). Furthermore no significant difference between either efficiency or salt recovery was found with and without density difference compensation with a high nor low hydraulic conductivity, which means no difference between cases 5A & 5B and 6A & 6B.

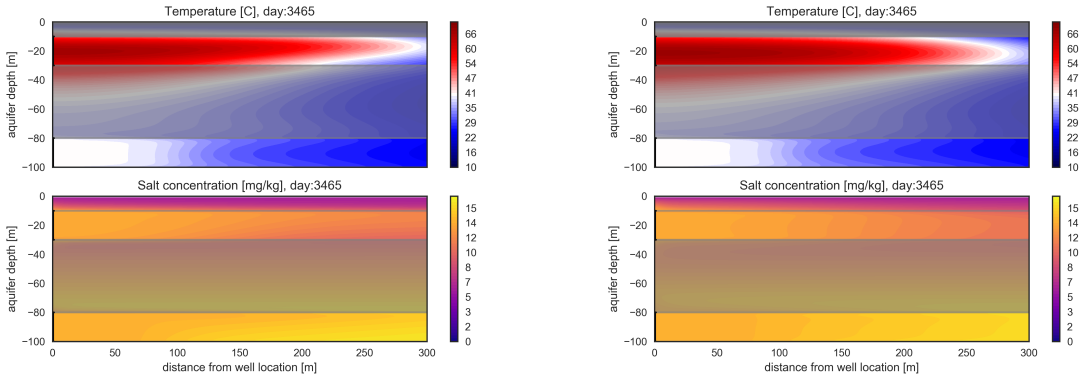

(a) Scenario 5B

(b) Scenario 6B

Figure 4.4: Difference in density driven flow due to K

4.3.5 Flow regime

A sinusoidal flow regime showed hardly any efficiency improvement with respect to the reference case with a block flow regime ($\Delta\varepsilon_H$=1.3%). A thick aquifer with a sinusoidal flow regime has exactly the same efficiency as a thick aquifer with a block flow regime.

5 Discussion

5.1 Simplifications

In the model some simplifications are made, which could have different results in comparison to reality. First of all the relation between temperature and density of water is nonlinear, but SEAWAT linearizes this. In the middle range of the linearization the density is assumed to be lower than in reality, like the plot in Figure 3.1 shows. So slightly cooled down water has a lower density in the model, which causes more upward flow, so more heat losses, and thus a lower efficiency than in reality.
Secondly, a simplification is made in the soil layers. What the model sees as the top of the soil, which means the temperature boundary is set to outside temperatures, is at a depth of 130m in reality. Figure 4.2 shows that this upper confining layer of 10m is not heated up by the HT-ATES system, because the upper layer is cooled down by the outside temperature, whilst the underlying confining layer is being warmed up. In reality the confining layer above the aquifer (of which the bottom is situated at a depth of 140m), will also heat up over the course of the years. This will lead to a higher efficiency in practice than the currently calculated efficiency. Another observation is, that over many years the heat conduction causes deeper layers to heat up as well. In reality there is another aquifer, the Formation of Oosterhout, situated at a 245m depth with a thickness of 150m [17], which may heat up. If this aquifer heats up significantly enough to retrieve more heat from this, a higher thermal efficiency coefficient could be achieved. Finally, the used flow regimes only take a seasonal variation of flow into account. In reality there will be a difference in demand between day and night, which means a difference in flow regime. This varying flow regime will cause a varying mixed convection ratio over the course of 24 hours, which might negatively or positively influence the efficiency and salt recovery.

5.2 Interfering systems within HT-ATES radius

With bigger volumes a higher efficiency and a better salt recovery can be achieved than with small volumes. However, a bigger volume means a bigger thermal radius, so the system will have a bigger influence on its environment. It might will have negative influence on other ATES systems an certain pipes. If the thermal radius becomes too big, more than one injection point by different wells could be chosen.

5.3 Influencing parameters

To check the influence of parameters on the system, one or two parameter(s) were changed with respect to the base scenario. The base scenario has a very thin aquifer in relation to the injection volume, this makes the HT-ATES system from the case study insensitive to density driven flow. So in this case study injection temperature and hydraulic conductivity show no significant impact on the salt recovery nor efficiency of the system. With simulations in a thick aquifer relative to injection volume, injection temperature and hydraulic conductivity might have a more significant influence on the system.

5.4 Effectiveness density difference compensation over time

To get better insight into the density difference compensation, various simulations were done with the optimum salinity of 39.1 kg/m^3. In addition to the base scenario, scenarios 7 and 11 were chosen, as scenarios with a thick aquifer have most potential for improvement. For a thick warm aquifer only (case 7D) the difference in efficiency compared to the theoretical optimum is

significantly lower ($\Delta\varepsilon_H$=-27.9%), 11D gets closer to the theoretical optimum ($\Delta\varepsilon_H$=-11.7%). With density difference compensation less density driven flow occurs than in the reference case, however the volume is not the same shape as the theoretical optimum. Figure C.1 and Figure C.2 in Appendix C show the temperature distribution of different cases for scenario 7 and 11. Generally the efficiency improves over the years, cases 7D and 11D however, are the only cases where the efficiency decreases with time, see Figure C.3 in C.
The decrease in efficiency over the years is caused by the reduction of the effectiveness of density difference compensation. Between every injection and extraction phase solute transport in the direction away from the well takes place. Due to thermal retardation, more solute transport takes place so the salt ends up further away from the well screen [8]. As can be seen in Figure 5.1, showing the heat and salinity distribution after extraction in year 10, a lot of salt stays behind at the top of the warm aquifers. Consequently, the warm well increases in salinity particularly where the hot water will be injected next. The extracted water from the warm well, which is the injected water in the next time step for the cold well, has a lower salinity than the salinity in the cold well. After this is injected the 'cold' well will become less saline. Over the years the injected water will have a lower density (due to decreased salinity), while the ambient groundwater in the warm well will have a increased density (due to increased salinity), resulting in density difference compensation becoming less effective over time.

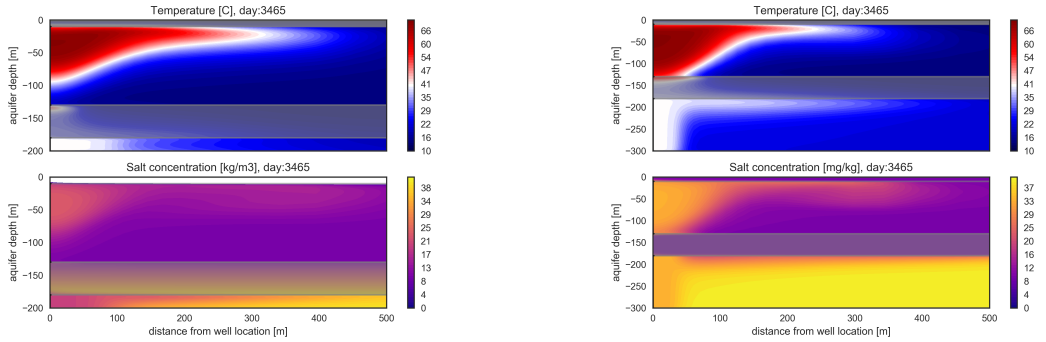

(a) Case 7D (b) Case 11D

Figure 5.1: Temperature and salt distribution before the extraction period of year 10

The decrease in efficiency can be enhanced by the interaction between the cold and warm well. When the cold well is situated in a thick aquifer, the hot injected water with a lower salinity will flow upwards and mix better with the water in the aquifer, like in Figure 5.1b. This density driven flow has a positive influence on the system, more water with a high salinity can be recovered. If the cold well would be situated in a thin aquifer, the water with a lower salinity will completely fill up the aquifer near the well screen, as is the case in Figure 5.1a. Now only water with a lower salinity will be recovered during the next cycle. As a result, the injection fluid for the hot water in the hot well will be significantly lower than the optimum salinity, and as a result more density driven flow will occur. This process will repeat over the cycles, causing the efficiency to rapidly decrease. Figure 5.2 shows that the salinity decreases more rapidly for the case when the cold well is situated in a thin aquifer (case 11D).

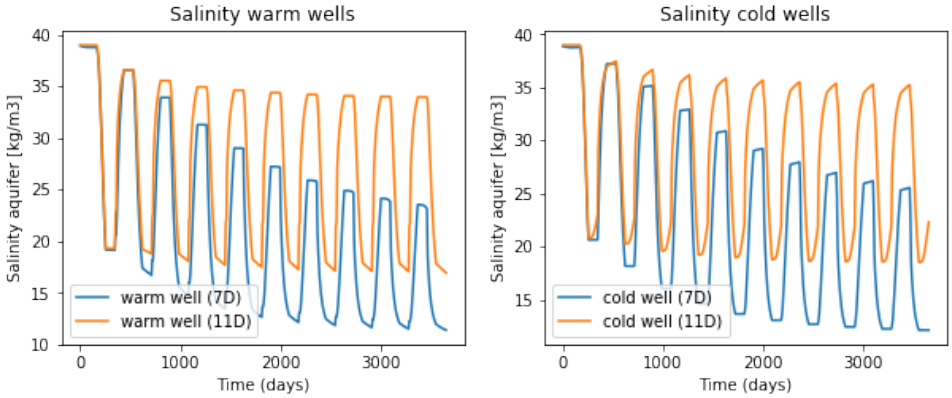

Figure 5.2: Salinity development in wells for thin and thick cold aquifer.

The extraction temperatures confirm the difference in efficiency, between scenarios 7 and 11. The extraction temperatures for the thin cold aquifer scenario (Figure C.6) are nearly equal for the theoretical optimum and the optimum density difference compensation in the first year. However in the tenth year the recovery temperatures are significantly lower. A thick cold aquifer stays closer to the extraction temperatures of the theoretical optimum, as can be seen in Figure C.7 in Appendix C. For scenario 1 all the different cases are nearly equal. Also, the efficiency hardly differs for the different cases of the reference scenario. Extraction temperatures for year 1 and year 10 for scenario 1, 7 and 11 are shown in Appendix C.

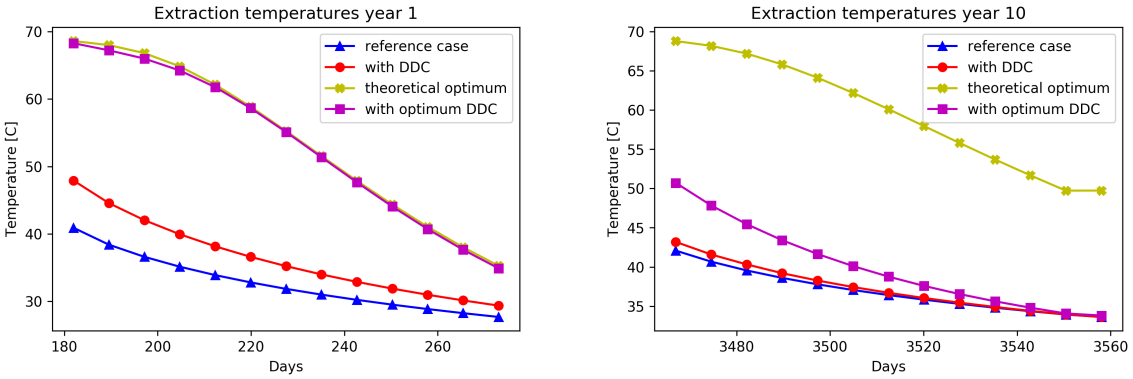

(a) Year 1 (b) Year 10

Figure 5.3: Extraction temperatures of scenario 7 for different cases

The efficiency of the case with two thick aquifer and optimum density difference compensation, is hardly higher than the reference case. So it is more than 10% lower than the theoretical optimum. This is caused by the increasing salinity at the top of the warm well, which makes the efficiency decrease over the years. It can be expected that the efficiency would not decrease over the years, when the salt would sink to the bottom of the aquifer. In future research could investigate a similar case with a higher injection temperature, and thus a higher salinity of the injection fluid. The higher the salinity of the injection fluid, the more likely it is to sink to the bottom of the aquifer after it has cooled down. For this scenario it can be expected that the efficiency can get significantly closer to the efficiency of the theoretical optimum.

6 Conclusion and Recommendations

The goal of this study was to get insight into the behaviour of a possible HT-ATES system on the campus of TU Delft with the injection of saline groundwater from deeper layers for storage in both less deep and less saline aquifers over several cycles.

6.1 Influencing parameters

The A/V ratio has the biggest influence on the salt recovery and efficiency of HT-ATES systems, this means that injection volume and aquifer thickness are the most influencing parameters. With optimum density difference compensation and a thick aquifer of both the 'cold' and warm well, the highest efficiency of 75.5% is achieved after 10 cycles, in this scenario the thickness of the 'cold' well aquifer has a positive influence on the efficiency.

6.2 Effect density difference compensation on efficiency

Density difference compensation has hardly any influence on the thermal recovery efficiency for the case study at TU Delft, because a very big volume is injected in a relatively thin aquifer, which causes conduction losses to dominate. A thin aquifer makes the system less sensitive to changes. The small density difference compensation used in the case study has no useful effect on efficiency in any scenario. HT-ATES systems with a thick aquifer are most sensitive to density driven flow. For the case with no density difference compensation (A), the lowest efficiency of 53.9% was found for a thick aquifer, this efficiency is significantly lower than the base scenario. However, the optimum density difference compensation shows most improvement for a thick aquifer, and the highest efficiency of 87.6% can be reached for theoretical optimum in a thick aquifer. Cases with thick aquifers and optimum density difference compensation are the only ones where the efficiency decreases over the years. 'Cold' aquifer thickness has a positive correlation with the effectiveness of density difference compensation over time.

6.3 Distribution of temperature

Not much upward flow occurs for any of the scenarios, except scenarios with a bigger aquifer thickness and a smaller volume (the scenarios with a small A/V). For scenarios with a big A/V the radius becomes very big, this causes a very big area of the underlying aquitard to heat up. For these scenarios there was no significant difference in heat distribution within the different cases, for cases with and without density difference compensation respectively, nor the theoretical optimum. For the other scenarios, with a smaller A/V ratio significant upward flow of the hot water bubble occurs. As a result the underlying aquitard hardly heats up. The optimum density difference compensation reduces the density driven flow, and a bigger hot volume can be maintained. For the theoretical optimum in a big aquifer, a perfect volume with a relatively small area can be achieved.

6.4 Salt recovery

The salt recovery has a negative correlation with salinity of the injection fluid and with aquifer thickness. A minimum salt recovery of 78.4% and maximum of 94.7% is found. For the scenarios with a small density difference compensation (case B) there is a strongly positive correlation between salt recovery and efficiency.

6.5 Distribution of salt

For the optimum density difference compensation in a thick aquifer, a substantial amount of salt stays at the top of the aquifer. When the 'cold' well is situated in a thin aquifer in this scenario, water with a lower salinity stays near the 'cold' well screen, when a thick 'cold' aquifer is used, water with a lower salinity floats to the top, so water with a high salinity can be extracted for the subsequent cycle.

6.6 Recommendations

To get a better insight in HT-ATES systems it is useful to carry out an extensive sensitivity analysis in further research. To gain more insight into the effects of varying flow regimes on the system, also day and night differences should be considered. Before implementation of the system, should investigated whether any aquifer between the warm and 'cold' well heats up significantly enough to retrieve more heat from this, and so a higher thermal efficiency coefficient can be achieved. Also, it should be investigated whether there are other ATES systems or pipes in the influencing area of the HT-ATES system.

References

[1] NASA Earth Obervatory. *Features*. URL: https://earthobservatory.nasa.gov/Features/WorldOfChange/decadaltemp.php.

[2] CE Delft. *Warmtevraag en -productie*. URL: http://www.ce.nl/ce/warmte_en_koeling/647.

[3] CE Delft. "Een klimaatneutrale warmtevoorziening voor de gebouwde omgeving". In: (2016).

[4] Union of concerned scientists. *How Thermal Energy Works*. URL: http://www.ucsusa.org/clean_energy/our-energy-choices/renewable-energy/how-geothermal-energy-works.html#.WbktGbIjGpo (visited on 2014).

[5] Hartog, N. et al. "Visie op warmtevoorziening". In: (2016).

[6] Schout, G. et al. "Analysis of recovery efficiency in high-temperature aquifer energy storage: a Rayleigh-based method". In: *Hydrogeology Journal* 22 (2014). An optional note, pp. 281–291.

[7] German Research Centre for Geosciences GFZ. *Underground storage*. URL: http://www.gfz-potsdam.de/en/section/geothermal-energy-systems/projects/geosolcool/project-details/underground-storage/ (visited on 09/30/2016).

[8] Van Lopik, J.H., Hartog, N., and Zaadnoordwijk, W.J. "The use of salinity contrast for density difference compensation to improve the thermal recovery efficiency in high-temperature aquifer thermal energy storage systems". In: *Hydrogeology Journal* (2016), pp. 1–17.

[9] SKB. "Cahier Bodemenergie, warm aanbevolen". In: (). An optional note, p. 26.

[10] Ruben Calje. "Future use of Aquifer Thermal Energy Storage below the historic centre of Amsterdam." MA thesis. TU Delft, 2010.

[11] Doughty, C. et al. "A dimensionless parameter approach to the thermal behavior of an aquifer thermal energy storage system". In: *Water Resources Research* (1982). An optional note.

[12] Schout, G., Drijver, B., and Schotting, R. "The influence of the injection temperature on the recovery efficiency of high temperature aquifer thermal energy storage: Comment on Jeon et al., 2015". In: *Energy* 103 (2016). An optional note, pp. 107–109.

[13] Ward, J. D., Simmons, C. T., and Dillon, P. J. "A theoretical analysis of mixed convection in aquifer storage and recovery: How important are density effects?" In: *Journal of Hydrology* 343 (Sept. 2007), pp. 169–186.

[14] Bloemendal, M. and Hartog, N. "Analysis of the impact of storage conditions on the thermal recovery efficiency of low-temperature ATES systems". In: *Geothermics* (2017). In press.

[15] Delft Aardwarmte Project. *Welcome to the website of the Delft Geothermal Project (DAP)*. URL: http://www.delftaardwarmteproject.nl/.

[16] Vincent Leclercq. "Enhancing the efficiency of High-Temperature storage by reducing the effect of density-driven flow". B.S. Thesis. TU Delft, 2017.

[17] Tim Hacking. "The Suitability of a High Temperature Aquifer Thermal Energy Storage on the TU-Delft Campus". B.S. Thesis. TU Delft, 2017.

[18] SolidWorks Help. *Coordinate Systems*. URL: http://help.solidworks.com/2013/english/solidworks/cworks/c_coordinate_systems.htm.

[19] Wikipedia. *Pearson Correlation Coefficient*. 2017. URL: https://en.wikipedia.org/wiki/Pearson_correlation_coefficient (visited on 10/09/2017).

A Model boundaries and parameters

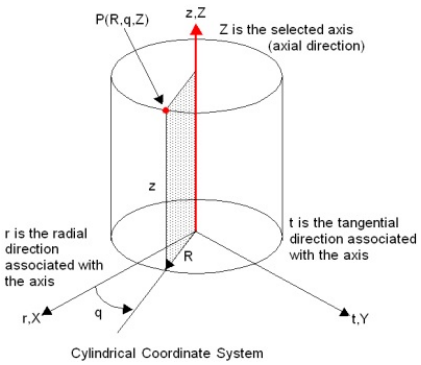

Figure A.1: Cylindrical coordinate system. (SolidWorks Help [18]).

These parameters are generally used for the simulations. For specific cases like the sensitivity analysis and in some of the cases other parameters are used and clearly stated in the general text.

In the general cases where efficiency is calculated, the model is run for 10 years, with time steps of 7 days, dz=1m, the simulation is started in winter.

Table A.1: Model boundaries

Model boundaries	**Value**	**Unit**
radius	300	[m]
aquifer thickness warm well	20	[m]
aquifer thickness 'cold' well	20	[m]
thickness middle aquitard	50	[m]
thickness overlying aquitard	10	[m]
thickness underlying aquitard	10	[m]
gridlayer thickness (dz)	1.0	[m]
dmin,dmax		[m]
upper boundary model	z = 0	[m]
lower boundary model	z = -110	[m]
size well	20	[m]

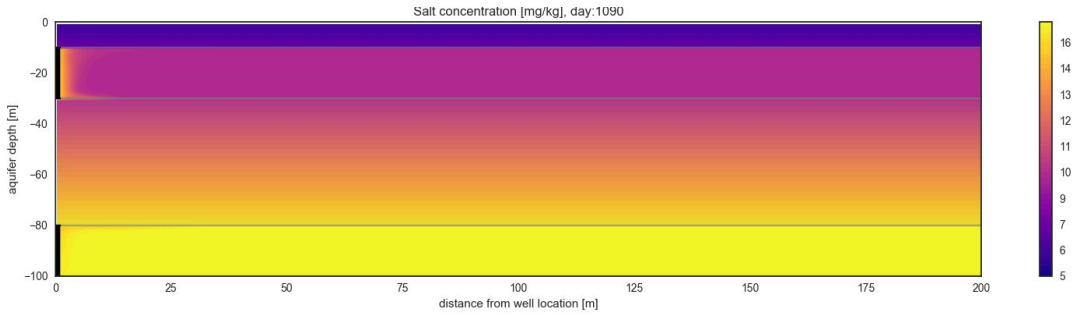

Figure A.2: Salinity distribution over depth.

Table A.2: Aquifer and aquitard properties

Aquifer and aquitard properties	**Value**	**Unit**
specific storage	$1{\cdot}10^{-5}$	$[m^{-1}]$
porosity	0.3	[-]
bulk density	2640	$[kg/m^3]$
heat capacity	710	$[J/m^3/K]$
thermal conductivity	3.0	[W/m/K]
thermal distribution coefficient	$1.697{\cdot}10^{-4}$	$[m^3{\cdot}kg]$
bulk thermal diffusivity	0.1566	$[m^2/d]$
horizontal hydraulic conductivity (aquifer)	55	[m/d]
vertical hydraulic conductivity (aquifer)	11	[m/d]
horizontal hydraulic conductivity (aquitard)	0.01	[m/d]
vertical hydraulic conductivity (aquitard)	0.002	[m/d]
salinity gradient	17	[mg/L/m]
ambient temperature (aquifer)	14.4	[°C]
ambient temperature (aquitard)	22.4	[°C]

Table A.3: HT-ATES properties

HT-ATES properties	**Value**	**Unit**
injection volume	1,400,000	$[m^3]$
injection temperature	70	[°C]

Table A.4: Groundwater properties

Groundwater properties	**Value**	**Unit**
heat capacity	4183	[J/kg/K]
thermal conductivity	0.61	[W/K/m]

Table A.5: Solute transport properties

Solute transport properties	**Value**	**Unit**
longitudinal dispersion	1	[m]
transversal dispersion	0.1	[m]
molecular diffusion	$1.00 \cdot 10^{-10}$	[m^2/d]

Table A.6: Overview scenarios

Scenario	T_{in} [°C]	V_{in} [m^3]	K_h [m/d]	K_v [m/d]	H_a warm [m]	H_a cold [m]	Flow function
1	70	$1.4 \cdot 10^6$	55	11	20	20	block
2	90	$1.4 \cdot 10^6$	55	11	20	20	block
3	50	$1.4 \cdot 10^6$	55	11	20	20	block
4	70	$2.5 \cdot 10^5$	55	11	20	20	block
5	70	$1.4 \cdot 10^6$	100	50	20	20	block
6	70	$1.4 \cdot 10^6$	10	1.0	20	20	block
7	70	$1.4 \cdot 10^6$	55	11	120	20	block
8	70	$1.4 \cdot 10^6$	55	11	50	20	block
9	70	$1.4 \cdot 10^6$	55	11	20	20	sinus
10	70	$1.4 \cdot 10^6$	55	11	120	20	sinus
11	70	$1.4 \cdot 10^6$	55	11	120	120	block

B Efficiency and salt recovery overview

		1. Base scenario	2. High T_{in}	3. Low T_{in}	4. Small V_{in}	5. Big K	6. Small K	7. Thick Ha (warm)	8. Medium Ha (warm)	9. Sinus flow	10. Thick Ha Sinus flow	11. Thick Ha (warm and cold)
A. Reference	*average* ε_H	71.78%	69.51%	74.71%	64.67%	70.41%	73.15%	51.30%	70.46%	71.16%	50.56%	51.34%
	ε_H *final year*	74.67%	72.71%	77.14%	67.69%	73.38%	75.95%	53.90%	73.53%	75.93%	53.90%	53.93%
	$\Delta\varepsilon_H$ (wrt scenario 1)	0.00%	-1.96%	2.47%	-6.98%	-1.29%	1.29%	-20.76%	-1.13%	1.26%	-	-20.74%
B. DDC TU Delft	*average* ε_H	71.94%	69.74%	74.81%	65.41%	70.74%	73.17%	52.89%	71.47%	71.28%		53.94%
	ε_H *final year*	74.77%	72.86%	77.19%	68.09%	73.57%	75.96%	54.61%	73.94%	76.03%		56.01%
	ε_S *warm well*	93.56%	93.23%	93.73%	90.69%	93.17%	93.63%	88.67%	91.33%	94.66%		83.96%
	$\Delta\varepsilon_H$ (wrt scenario 1)	0.00%	-1.91%	2.43%	-6.68%	-1.20%	1.19%	-20.16%	-0.82%	1.26%	-	-18.76%
	$\Delta\varepsilon_H$ (wrt case A)	0.10%	0.15%	0.06%	0.41%	0.20%	0.01%	0.71%	0.41%	0.10%	-	2.08%
	$\Delta\varepsilon_S$ (wrt scenario 1)	0.00%	-0.33%	0.17%	-2.87%	-0.39%	0.07%	-4.89%	-2.23%	1.10%	-	-9.60%
C. Theoretical optimum	*average* ε_H	72.69%			71.95%			84.48%			82.25%	84.42%
	ε_H *final year*	75.40%			74.65%			87.28%			87.59%	87.17%
	$\Delta\varepsilon_H$ (wrt scenario 1)	0.00%	-	-	-0.75%	-	-	11.88%	-	-	12.19%	11.77%
	$\Delta\varepsilon_H$ (wrt case A)	0.74%	-	-	6.96%	-	-	33.37%	-	-	33.69%	33.24%
D. Optimum DDC	*average* ε_H	72.39%						64.92%				76.15%
	ε_H *final year*	75.10%						59.33%				75.47%
	ε_S *warm well*	86.68%						78.44%				80.35%
	ε_H *first year*							76.66%				76.67%
	$\Delta\varepsilon_H$ (wrt scenario 1)	0.00%	-	-	-	-	-	-15.77%	-	-	-	0.37%
	$\Delta\varepsilon_H$ (wrt case A)	0.43%	-	-	-	-	-	5.42%	-	-	-	21.54%
	$\Delta\varepsilon_H$ (wrt case C)	0.30%	-	-	-	-	-	-27.95%	-	-	-	-11.70%
	$\Delta\varepsilon_S$ (wrt scenario 1)	0.00%	-	-	-	-	-	-8.24%	-	-	-	-6.34%
	$\Delta\varepsilon_S$ (wrt case B)	-6.88%	-	-	-	-	-	-10.23%	-	-	-	-3.61%

Figure B.1

C Results: figures

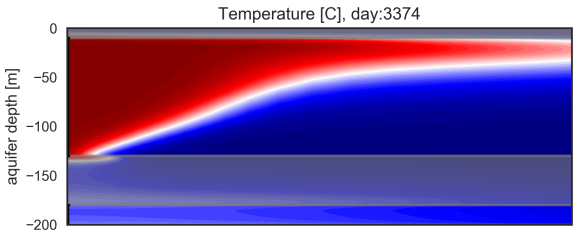

(a) Reference case (7A)

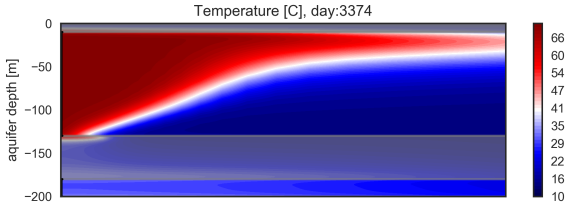

(b) DDC TU Delft (7B)

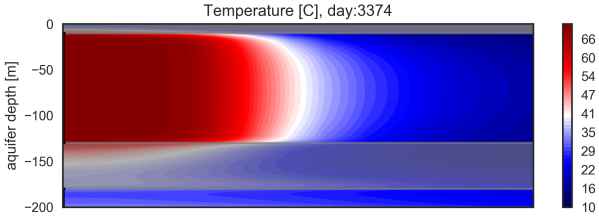

(c) Theoretical optimum (7C)

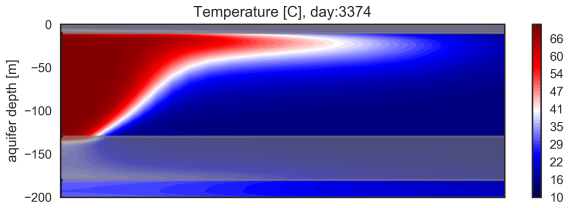

(d) Optimum DDC (7D)

Figure C.1: Temperature distribution scenario 7

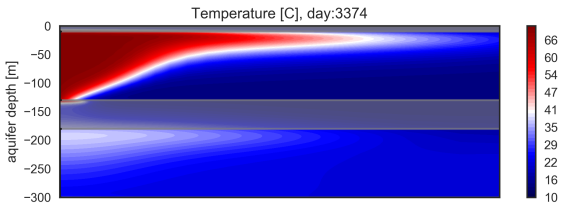

(a) Reference case (11A)

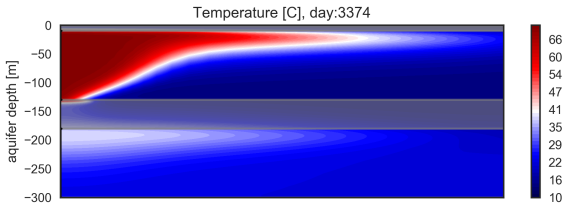

(b) DDC TU Delft (11B)

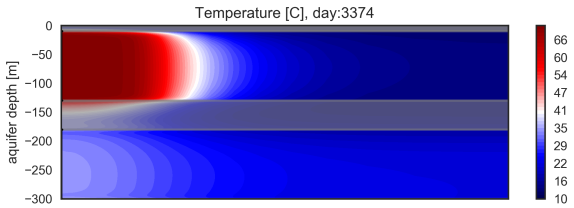

(c) Theoretical optimum (11C)

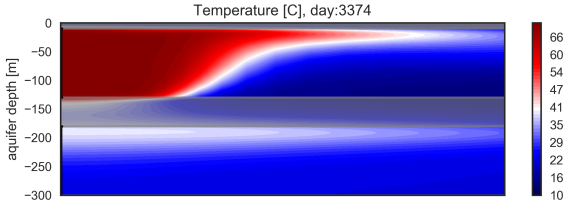

(d) Optimum DDC (11D)

Figure C.2: Temperature distribution scenario 11

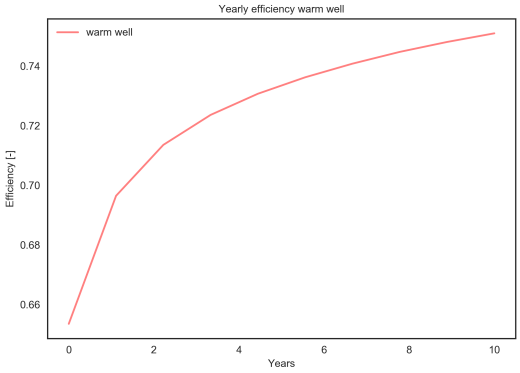

(a) Scenario 1D

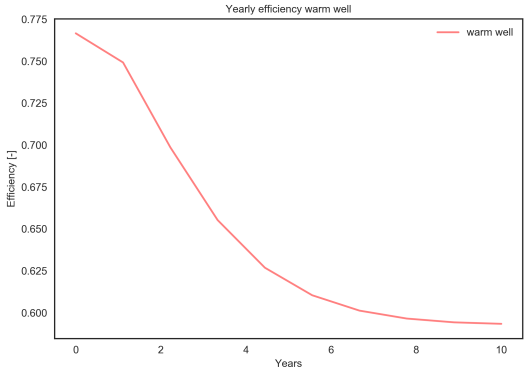

(b) Scenario 7D

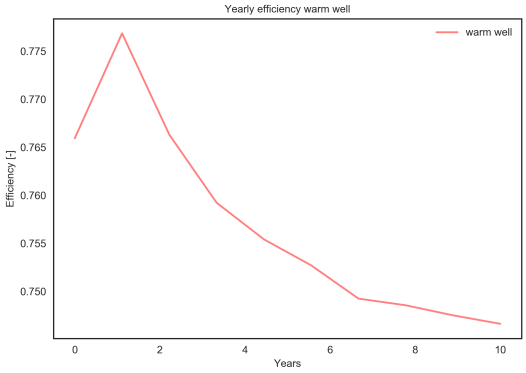

(c) Scenario 11D

Figure C.3: Efficiency development over 10 years

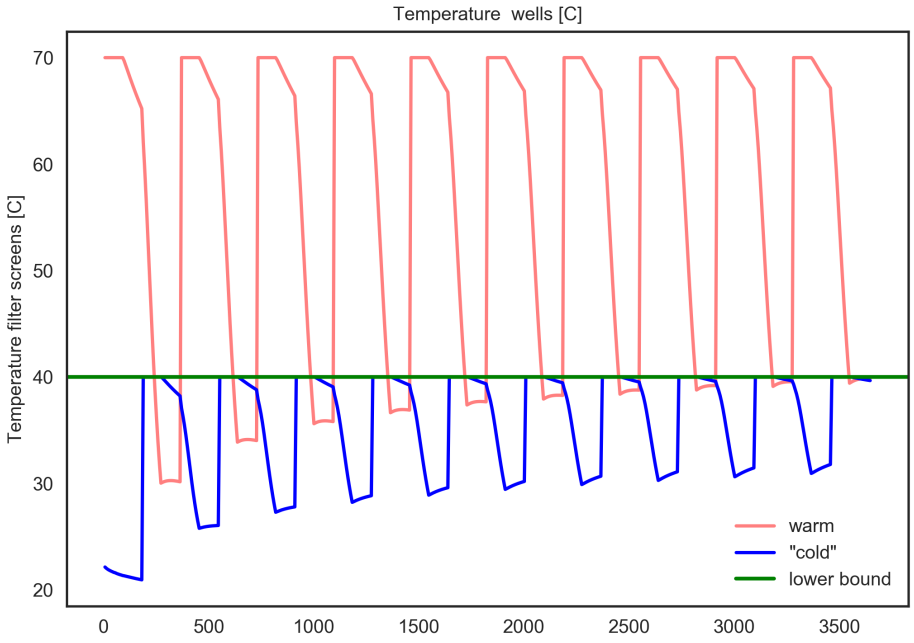

Figure C.4: Temperature wells for base scenario (1A)

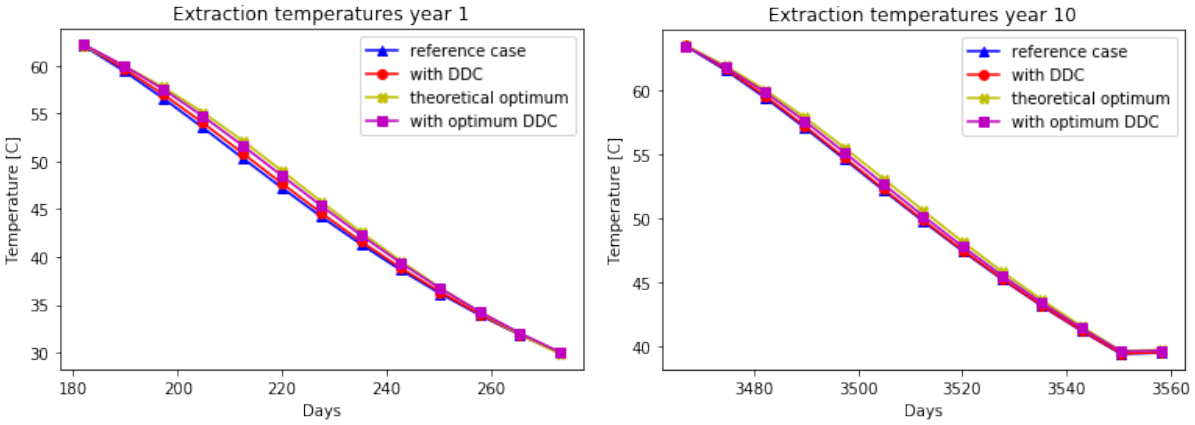

(a) Year 1 (b) Year 10

Figure C.5: Extraction temperatures of scenario 1 for different cases

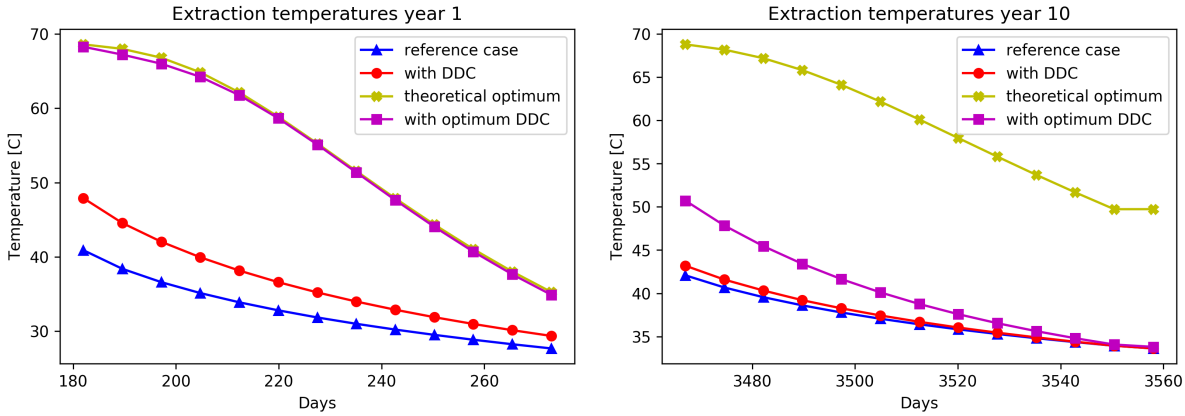

(a) Year 1 (b) Year 10

Figure C.6: Extraction temperatures of scenario 7 for different cases

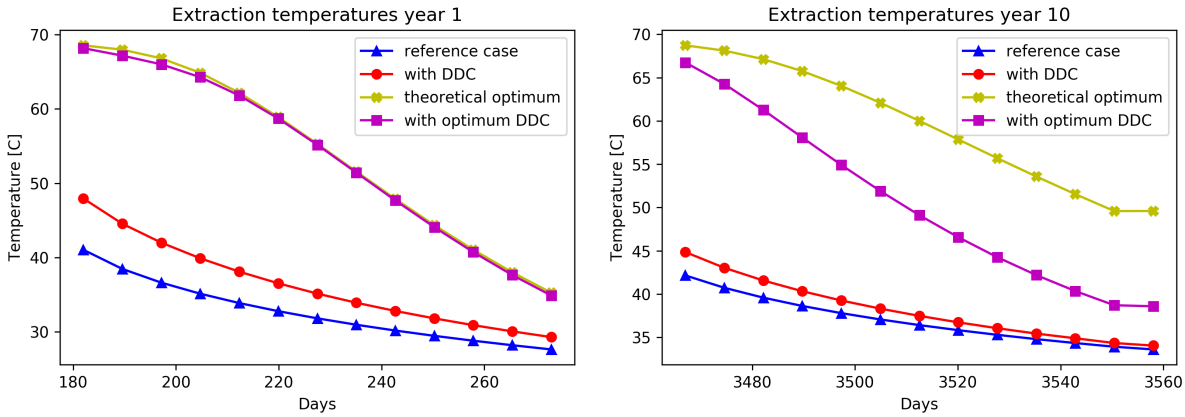

(a) Year 1 (b) Year 10

Figure C.7: Extraction temperatures of scenario 11 for different cases

D Formulas

D.0.1 Pearson correlation coefficient

The correlation coefficient between two random variables X and Y is defined as [19]:

$$\rho(X,Y) = \frac{\mathbf{Cov}(X,Y)}{\sigma_X \sigma_Y} = \frac{\mathbf{Cov}(X,Y)}{\sqrt{\mathbf{Var}(X)\mathbf{Var}(Y)}} \tag{D.1}$$

with:
Cov is the covariance
σ_X is the standard deviation of X
σ_Y is the standard deviation of Y